



SODs, DNA binding and cleavage studies of new Mn(III) complexes with 2-((3-(benzyloxy)pyridin-2-ylimino)methyl)phenol

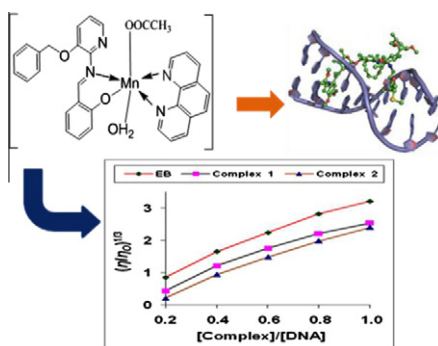
L. Shivakumar, K. Shivaprasad, Hosakere D. Revanasiddappa*

Department of Chemistry, University of Mysore, Manasagangotri, Mysore 570 006, Karnataka, India

HIGHLIGHTS

- ▶ Synthesis of new Schiff base and its Manganese(III) complexes.
- ▶ Spectral and thermal characterization of the synthesized compounds.
- ▶ SODs activity.
- ▶ Antimicrobial activity of the synthesized complexes.
- ▶ DNA binding properties and oxidative induced supercoiled DNA cleavages of the complexes.

GRAPHICAL ABSTRACT



ARTICLE INFO

Article history:

Received 16 October 2012

Received in revised form 8 January 2013

Accepted 10 January 2013

Available online 31 January 2013

This work is dedicated to Dr. P.G. Ramappa, Former Professor of Inorganic Chemistry, University of Mysore, on his 75th birth anniversary.

Keywords:

Mn(III) complexes
SOD mimic activity
DNA binding
Oxidative DNA cleavage
Antimicrobial activity

ABSTRACT

Newly synthesized ligand [2-((3-(benzyloxy)pyridin-2-ylimino)methyl)phenol] (Bpmp) react with manganese(II) to form mononuclear complexes $[\text{Mn}(\text{phen})(\text{Bpmp})(\text{CH}_3\text{COO})(\text{H}_2\text{O})]\cdot 4\text{H}_2\text{O}$ (**1**), (phen = 1, 10-phenanthroline) and $[\text{Mn}(\text{Bpmp})_2(\text{CH}_3\text{COO})(\text{H}_2\text{O})]\cdot 5\text{H}_2\text{O}$ (**2**). These complexes were characterized by elemental analysis, IR, ^1H NMR, Mass, UV-vis spectral studies. Molar conductance and thermogravimetric analysis of these complexes were also recorded. The *in vitro* SOD mimic activity of Mn(III) complexes were carried out and obtained with good result. The DNA-binding properties of the complexes **1** and **2** were investigated by UV-spectroscopy, fluorescence spectroscopy and viscosity measurements. The spectral results suggest that the complexes **1** and **2** can bind to Calf thymus DNA by intercalation mode. The cleavage properties of these complexes with super coiled pUC19 have been studied using the gel electrophoresis method, wherein both complexes **1** and **2** displayed chemical nuclease activity in the absence and presence of H_2O_2 via an oxidative mechanism. All the complexes inhibit the growth of both Gram positive and Gram negative bacteria to competent level. The MIC was determined by micro-titer method.

© 2013 Elsevier B.V. All rights reserved.

Introduction

Schiff bases belong to a class of organic compounds which have potential as anticancer drugs, indeed the activity of these compounds increase when they complex with metal ions [1]. Coordination chemistry of manganese in various oxidation states has long

been investigated as an area of considerable interest in inorganic biochemistry [2]. Schiff bases derived from salicylaldehyde and various amines have been extensively used to synthesize many complexes of manganese(III) [3–5]. Mn-Salen complexes have been exploited as a catalyst for reactions [6,7], models for catalytic scavengers (hydrogen peroxide and superoxide) [8], protective activity in various experimental disease models like EUK-8 (*in vivo*) [9,10]. Similar to Fe(III), the high spin Mn(III) is a trivalent cation and is classified as a hard Lewis acid by virtue of its high charge density.

* Corresponding author. Tel.: +91 821 2419669; fax: +91 821 2419363.

E-mail address: hdrevasiddappa@yahoo.com (H.D. Revanasiddappa).

In contrast to Mn(II), Mn(III) forms stable complexes with hard donor atoms, such as oxygen donors [11].

The investigation of biological properties of Schiff base complexes of Mn(III) have received less attention in comparison to the corresponding Mn(II) complexes. A large number of Schiff base complexes of manganese(III) find important roles in metalloenzymes, redox and non-redox proteins [12]. A few reports on the antimicrobial activity of Mn(III) complexes have been found in the literature [13,14]. The DNA interaction of a number of manganese complexes with different functionalized Salen derivatives has been investigated in literature [15–17]. These studies have indicated that while some complexes bind DNA avidly, others induce effective DNA scission *via* a redox process.

Reactive oxygen species (ROS) like the superoxide radical (O_2^-), formed following a one-electron reduction of molecular oxygen. Superoxide dismutases (SODs) are metalloenzymes that catalyze the conversion of superoxide radical (O_2^-) to oxygen (O_2) and hydrogen peroxide (H_2O_2) at rates approaching the diffusion controlled limit [18]. Therefore, they play a crucial role in protecting biological systems against the damage mediated by this deleterious radical. SODs, is in fact one of the first line ROS-defense enzymes in cells whose role is becoming increasingly important as more pathological and disease states are discovered to be linked with oxidative damage [19]. Many studies on the reactivity of the native SODs enzymes and low molecular weight manganese(II,III) based SOD mimetic (SODm) towards superoxide have been reported [20]. Manganese has been the preferred metal for the development of SODm complexes, due to its low toxicity compared to the other metals [21]. Additionally, it has been shown that high intracellular manganese concentrations can provide protection against oxidative stress [22].

Although some important classes of SODm have proven to be effective in clinical trials in manipulating a variety of disease states related to reactive oxygen and nitrogen species, the key mechanisms behind their bioactivity are still unclear [23]. It has been documented in the literature that native SODs enzyme also interact with DNA and exhibit nuclease activity [24,25]. This prompted us to study the DNA interaction as well as nuclease activity of manganese complexes having SODs activity.

Therefore, in this paper the authors have tried to present manganese complexes represents manganese-SODs for a treatment of the oxidative stress like disease, using indirect spectrophotometric detection of superoxide decomposition method in aqueous media. The structure of newly synthesized Schiff base and its manganese(III) complexes were accomplished by spectral characterization *viz.*, IR, UV–vis, mass, and elemental analysis and thermogravimetric analysis. Also DNA interactions of the two complexes with calf-thymus DNA (CT-DNA) were investigated using UV–vis absorption titration, fluorescence spectra and viscosity measurements. In addition, their oxidative-cleavage reactions with pUC19 supercoiled plasmid DNA were elucidated by gel electrophoresis. The complexes were also tested for their *in vitro* antimicrobial activity against some Gram positive and Gram negative strains using the paper disc diffusion method. Microtiter method was used to determine MIC values.

Experimental

Chemicals

All reagents were procured from Merck and Sigma Aldrich Co. and used without further purification unless specially noted. The solvents used for spectroscopic studies were purified by standard procedures [26]. Calf Thymus (CT) and Supercoiled (SC) pUC19 DNA were purchased from Genei, Bangalore (India). Tris–HCl

buffer solution was prepared using deionized, sonicated triply-distilled water.

Physical measurement

Elemental analysis was carried out on an Elemental Vario EL elemental analyzer. 1H NMR spectra were recorded on a Bruker AV-400 MHz FT NMR spectrometer in $CDCl_3$. The electro-spray ion mass spectra (ESIMS) were recorded on API 2000 Applied Bio-system triple quadrupole mass spectrometer. The solution was introduced into the ESI source through a syringe pump at the rate 5 $\mu L/min$. The molar conductance data were recorded in 10^{-3} M DMF solution at room temperature using an Elico CM-180 conductometer. The cell constant of the conductivity cell used was 0.5 cm^{-1} . Infrared spectra were recorded in the range $4000\text{--}400\text{ cm}^{-1}$ on a Jasco FT/IR-4100 Series FT-IR spectrometer by Nujol mull method. Electronic spectra were obtained with a Hitachi U-2000, recording spectrophotometer in DMF solution at concentration of 10^{-3} M. Magnetic measurement were carried out by the Gouy method at room temperature ($28 \pm 2^\circ C$) using $Hg[Co(SCN)_4]$ as the calibrant. Thermogravimetric and Differential thermal analysis were performed by Universal V4.3A TA Instruments. Fluorescence spectra were recorded on a Shimadzu RF-5301pc spectrofluorimeter. The metal contents in the complexes were determined by literature method [27].

Synthesis of the ligand (Bpmp)

A solution of salicylaldehyde (0.245 g, 2 mmol) in methanol (20 mL) was added to a methanolic solution (30 mL) of 3-(benzyl-oxy)pyridin-2-amine (0.400 g, 2 mmol). The reaction mixture was heated under reflux for 8 h. The solution was cooled and left to stand for the evaporation, after few days reddish brown colored crystals of Bpmp were obtained in a good yield (Yield = 0.522 g, 81%). m.p: $90^\circ C$; Anal. Calcd. for $C_{19}H_{16}N_2O_2$: C, 74.98; H, 5.30; N, 9.20; O, 10.51; Found: C, 74.92; H, 5.28; N, 9.12; O, 10.46%; FT-IR (Nujol) (ν_{max}/cm^{-1}): 1670 (HC=N), 3613 (Ph–OH); ESI-MS, m/z : 305 $[M + 1]^+$; 1H NMR ($CDCl_3$, 300 MHz, δ ppm): 5.14 ($-CH_2-$ –O), 10.54 (s, Ph–OH), 9.18 (s, HC=N), 7.26–6.56 (m, Ar–H).

Synthesis of the complex (1) $[Mn(phen)(Bpmp)(CH_3COO)(H_2O)] \cdot 4H_2O$

A methanolic solution (10 mL) containing 1.0 mmol (0.245 g) quantity of $Mn(CH_3COO)_2 \cdot 4H_2O$ was reacted with 1.0 mmol (0.198 g) of the heterocyclic base (phen) in 10 mL MeOH under stirring at $40^\circ C$ for 0.5 h. The resulting solution was then reacted with 1.0 mmol (0.305 g) of Bpmp taken in 10 mL hot MeOH. The mixture was refluxed with stirring for 10 h and cooled. After slow evaporation at room temperature, a light yellowish brown microcrystalline product was deposited, collected with filtration, washed with methanol and dried.

Complex 1: Yield: (73%). m.p: $>300^\circ C$. Anal. Calc. for $[C_{33}H_{36}MnN_4O_9]$ (%): C, 57.64; H, 5.28; N, 8.15; O, 20.94; Found: C, 57.04; H, 5.20; N, 8.10; O, 20.83; FT-IR (Nujol) (ν_{max}/cm^{-1}): 3395, (H_2O); 1282, $\nu(COO^-)_{sy}$; 1580 $\nu(COO^-)_{asy}$; 561, 543 (M–N); 442 (M–O). ESI-MS, m/z : 688 $[M + 1]^+$. Conductance (Λ , $ohm^{-1} cm^2 mol^{-1}$), 19.2; μ_{eff} (BM), 4.73.

Synthesis of the complex (2) $[Mn(Bpmp)_2(CH_3COO)(H_2O)] \cdot 5H_2O$

The complex was prepared by stirring a MeOH solution (25 mL) of Bpmp (2 mmol, 0.61 g) and adding successively a MeOH solution (25 mL) of $Mn(CH_3COO)_2 \cdot 4H_2O$ (1 mmol, 0.245 g) under reflux. The initial yellow color of the solution rapidly changed to brown. After 24 h of stirring at room temperature slow evaporation of solvent

lead to deposition brown compounds. The products were collected by filtration and washed with ethanol–diethyl ether mixture (1:1).

Complex 2: Yield: (64%). m.p >300 °C. Anal. Calc. for $[\text{C}_{40}\text{H}_{45}\text{MnN}_4\text{O}_{12}]$ (%): C, 57.97; H, 5.47; N, 6.76; O, 23.17; Found: C, 56.88; H, 5.51; N, 6.28; O, 22.93; FT-IR (Nujol) ($\nu_{\text{max}}/\text{cm}^{-1}$): 3412, (H_2O); 1285, $\nu(\text{COO}^-)_{\text{sy}}$; 1585 $\nu(\text{COO}^-)_{\text{asy}}$; 554, 541 (M–N); 436 (M–O). ESI-MS, m/z : 829 $[\text{M} + 1]^+$. Conductance (Λ , $\text{ohm}^{-1} \text{cm}^2 \text{mol}^{-1}$), 15.9; μ_{eff} (BM), 4.95.

Superoxide dismutase activity

SOD activity of the complexes 1 and 2 were evaluated according to the reported method [28]. This *in vitro* method is based on the ability of tested compounds (1 mg/mL, 4% DMSO solution) to inhibit the reduction of nitro blue tetrazolium (NBT) (0.3 mL, 300 μM) by superoxide radical O_2^- generated by the phenazine metho sulfate (PMT) (0.1 mL, 186 μM) with NADH (0.2 mL, 780 μM) in phosphate buffer pH 7.8, of total volume 3 mL. The extent of NBT reduction was followed spectrophotometrically by measuring the absorbance at 560 nm. Each experiment was performed in duplicate and the SOD activity has been defined as the concentration of the tested compound for the 50% inhibition of the NBT reduction (IC_{50} value) by superoxide produced.

DNA binding and cleavage activity

Electronic absorption titration

All spectroscopic titrations were carried out in 5 mmol L⁻¹ Tris–HCl buffer (pH 7.1) containing 50 mmol L⁻¹ NaCl at room temperature. A solution of CT–DNA in the buffer gave a ratio of UV absorbance at 260 and at 280 nm of 1.84:1, indicating that the DNA was sufficiently free of protein [29]. The concentration of DNA was estimated from its absorption intensity at 260 nm with a known molar absorption coefficient value of 6600 M⁻¹ cm⁻¹ [30]. Stock solutions were stored at 4 °C and used within 4 days. Before adding CT–DNA to complexes 1 and 2, complexes were dissolved in less than 4% DMSO: H₂O. Titration experiments were performed by a fixed complex concentration (50 μM) while varying the concentration of the CT DNA from 0 to 300 μM . While measuring the absorption spectra, equal quantity of CT DNA was added to both the complex solution and the reference solution to eliminate the absorbance of CT DNA itself. The complex–DNA solutions were allowed to equilibrate for 10 min before spectra were recorded. The intrinsic binding constant (K_b) for the interaction of the complexes with CT DNA was determined from a plot of $[\text{DNA}]/(\epsilon_a - \epsilon_f)$ versus $[\text{DNA}]$ using absorption spectral titration data [31] and the following equation,

$$[\text{DNA}]/(\epsilon_a - \epsilon_f) = [\text{DNA}]/(\epsilon_b - \epsilon_f) + 1/K_b(\epsilon_b - \epsilon_f)$$

where $[\text{DNA}]$ is the concentration of DNA, the apparent absorption coefficients ϵ_a , ϵ_f and ϵ_b correspond to $A_{\text{obsd}}/[\text{complex}]$, the extinction coefficient for the free metal complex and the extinction coefficient for the metal complex in the fully bound form, respectively. The K_b value is given by the ratio of the slope to the intercept.

Fluorescence spectral study

The relative binding of the ternary complexes to CT DNA was studied by fluorescence spectral method using EB (Ethidium Bromide) bound CT DNA solution in Tris–HCl/NaCl buffer (pH 7.2). Emission intensity measurements were carried out on a Shimadzu RF-5301pc spectrofluorometer with a 1 cm quartz cell. Tris buffer was used as the blank to make preliminary adjustments. For all fluorescence measurements, the entrance and exit slits were maintained at 10 nm each. All the experiments were measured after 5 min at a constant room temperature, 302 K. Fluorescence intensities at 545 nm (376 nm excitation) were measured at different

complex concentrations. DNA was pretreated with EB in the ratio $[\text{DNA}]/[\text{EB}] = 1$ for 30 min at 27 °C. The metal complexes with the increasing concentration (0–50 μM) were then added to the DNA–EB (50 μM) mixture and their effect on the emission intensity was measured.

Viscosity measurements

Viscosity measurements were carried out with an Ubbelohde viscometer maintained at a constant temperature of 28.0 ± 0.1 °C in a thermostated bath. DNA samples of ca. 200-bp average length were prepared by sonication in order to minimize complexities arising from DNA flexibility [32]. The concentration of DNA was 200 μM , the EB and complex concentrations were varied from 0 to 200 μM and the flow times were measured with a digital timer. EB and each sample were tested three times to get an average calculated flow time. Data were presented as $(\eta/\eta_0)^{1/3}$ versus binding ratio [33], where η is the viscosity of DNA in the presence of complex, η_0 being the viscosity of free DNA solution alone. The viscosity values were calculated from the observed flow time of CT–DNA containing solutions (t) duly corrected for that of the buffer alone (t_0), $\eta = (t - t_0)/t_0$.

Oxidative DNA cleavage efficiency

The DNA cleavage activity of the metal complexes was studied by agarose gel electrophoresis. Supercoiled plasmid pUC19 DNA (30 μM) was dissolved in a 50 mM (Tris–HCl) buffer (pH 7.2) containing 50 mM NaCl and added to the different concentration of complexes (100, 200, 300 and 400 μM) prepared in less than 4% DMSO:H₂O. The mixtures were incubated at 37 °C for 24 h and then mixed with the loading buffer (2 μL) containing 25% bromophenol blue, 0.25% xylene cyanol and 30% glycerol. Each sample (5 μL) was loaded into 0.8% w/v agarose gel. Electrophoresis was undertaken for 1 h at 50 V in Tris–acetate–EDTA (TAE) buffer. The gel was stained with EB for 5 min after electrophoresis, and then photographed under UV light. The proportion of DNA in each fraction was quantitatively estimated from the intensity of each band with the Alpha Innotech Gel documentation system (Alphamager 2200). To enhance the DNA cleaving ability by the complexes, hydrogen peroxide (100 μM) was added into each complex (400 μM). Moreover, the cleavage mechanism was further investigated by using scavengers for the hydroxyl radical species (4 μL , DMSO) and the singlet oxygen species (100 μM , NaN_3). All experiments were carried out in triplicate, under the same conditions. Assays in the presence of the minor groove binder distamycin (8 μM) and the major groove binder methyl green (2.5 μL of a 0.01 mg/mL solution) were also performed.

Antimicrobial activities

The complexes and ligand were tested for their *in vitro* antibacterial activity against *Escherichia coli*, *Staphylococcus aureus*, *Xanthomonas vesicatoria* and *Ralstonia solanacearum* strains. Initial screening of compounds was performed by following disc diffusion method. Suspensions in sterile distilled water from 24 h cultures of microorganisms were adjusted to 0.5 McFarland. Muller–Hinton Petri dishes of 90 mm were inoculated using these suspensions. Paper disks (5 mm in diameter) containing 100 μL of the substance to be tested (at a concentration of 2 mg/mL in DMF) were placed at the edge of the petri plates containing nutrient agar (NA). One 5 mm diameter agar disc of test organism from a 1 week old NA culture was placed in the center of the plate. Incubation of the plates was done at 37 °C for 24 h. Reading of the results was done by measuring the diameters of the inhibition zones generated by the tested substances, using a ruler. Chloramphenicol was used as a reference substance.

The *in vitro* anti-fungal assay was performed by the disc diffusion method. The complexes and ligand were tested against the fungi *Aspergillus niger* and *Aspergillus flavus*, cultured on potato dextrose agar as medium. In a typical procedure, a well was made at the center on the agar medium inoculated with the fungi. The well was filled with the test solutions (100 μL) using a micropipette and the plate was incubated at 37 $^{\circ}\text{C}$ for 72 h. During this period, the test solution diffused and the growth of the inoculated fungi was affected. The inhibition zone developed on the plate was measured. Fluconazole was used as a reference compound.

The prepared compounds were further used to determine minimum inhibitory concentration (MIC) in 96 well, sterile, flat bottom microtiter plates, based on broth microdilution assay, which is an automated colorimetric method, uses the absorbance (optical density) of cultures in a microtiter plates [34]. Each well of microtiter plates was filled with 200 μL of nutrient broth/potato dextrose broth, 1 μL of test organism and 15 μL of different concentration of selected compounds. For bacteria and fungi the microtiter plates were incubated at 35 ± 2 $^{\circ}\text{C}$ for 24 h. After the incubation period, the plates were read at 610 nm using ELISA reader (ELX 800 MS, Biotek instruments, Inc. USA). MIC, which was determined as the lowest concentration of compound inhibiting the growth of the organism, was determined based on the optical density.

Results and discussion

Chemistry

The synthesis of Bpmp involves the addition of a solution of salicylaldehyde in methanol to a stirred methanolic solution of 3-benzoyloxy pyridin-2-ylamine in a 1:1 ratio. The level of the purity of Bpmp has been checked by running TLC on a silica gel coated plate using EtOAc–EtOH (6:4, v/v) as the mobile phase. The structure of ligand is characterized by IR, ^1H NMR, mass and UV spectra. The reaction of the ligands Bpmp/o-phen and $\text{Mn}(\text{CH}_3\text{COO})_2 \cdot 4\text{H}_2\text{O}$ in different ratio produced the mononuclear complexes **1** and **2**. Bpmp and its complexes **1** and **2** are insoluble in water, dichloromethane, ethyl ether and soluble in common polar organic solvents. The structures of complexes were characterized by elemental analysis, molar conductivities, IR, UV spectra, mass and thermogravimetric analysis. The elemental analysis data of the Bpmp and its metal complexes agree well with the proposed structure (Fig. 1). The synthesis, spectroscopic and analytical data of prepared manganese complexes are presented in the Experimental Section. The molar conductivities of complexes **1** and **2** in DMF are found to be 19.2 and 15.9 $\text{ohm}^{-1} \text{cm}^2 \text{mol}^{-1}$, respectively, which indicate that these complexes are neutral and non-electrolytes [35]. The relative low molar conductivities show that these complexes are stable in solution. Both the ligand and its complexes are very stable at room temperature in the solid state.

NMR spectra

^1H NMR spectral data of the ligand in CDCl_3 confirms the proposed structure of the ligand (Fig. 2). The sharp signal at δ 5.14 ppm in the spectra of Bpmp is assigned to the ($-\text{CH}_2-\text{O}$) methylene group, allied with the benzene ring. The free ligand spectrum shows a sharp signal at δ 9.18 ppm is assigned to the azomethine ($-\text{CH}=\text{N}-$) moiety [36]. The ^1H NMR spectrum of ligand shows a broad singlet at δ 10.54 ppm due to phenolic $-\text{OH}$ proton [37]. The spectrum also shows the multiple bands in the region δ 7.26–6.56 ppm, assigned for the aromatic ring protons.

IR spectra

The IR spectra of Bpmp and its complexes were presented in Figs. S1–S3. The IR spectral data of the Bpmp show a medium intensity absorption band at 3613 cm^{-1} which is attributed to the phenolic $\nu(\text{OH})$ stretching vibration. The phenolic C–O stretching can also be observed at 1286 cm^{-1} range. These bands are disappeared in complexes indicating that the ligand is coordinated to metal through deprotonated hydroxyl group [38]. The high intensity band at 1670 cm^{-1} appeared which is attributed to the $\nu(\text{CH}=\text{N})$ vibration of the ligand, and it disappeared upon coordination with metal ion. The presence of medium intensity bands in $2600\text{--}2700 \text{ cm}^{-1}$ region indicates the existence of C–H group of the ligand. The bands in the range $3370\text{--}3420 \text{ cm}^{-1}$ and 1620 cm^{-1} are attributable to O–H stretching and bending of coordinated water ligands or water of crystallization [39,40]. Ligand coordination to the manganese center in **1** and **2** is confirmed by two bands appearing about $576\text{--}543$ and $468\text{--}436 \text{ cm}^{-1}$, attributable to $\nu(\text{Mn}-\text{N})$ and $\nu(\text{Mn}-\text{O})$ [41], respectively. The IR spectra of the acetate complexes **1** and **2** show an absorption band in the region $1574\text{--}1590 \text{ cm}^{-1}$ which is assigned to $\nu(\text{COO}^-)$ asymmetric stretching of acetate ion and another in the region $1274\text{--}1295 \text{ cm}^{-1}$ and which can be assigned to $\nu(\text{COO}^-)$ symmetric stretching vibration of acetate ion. A difference between ($\nu_{\text{as}} - \nu_{\text{s}}$) is around $300\text{--}295 \text{ cm}^{-1}$ which is greater than 144 cm^{-1} indicates the unidentate coordination of the acetate ion with the central metal ion [42].

Electronic spectra and magnetic measurements

The UV–vis spectra of the ligand and its manganese(III) complexes in DMF were recorded in the region of 800–200 nm. All the complexes show similar electronic spectra to those previously reported for related other manganese(III) complexes [43]. The spectrum of all the d^4 manganese(III) complexes in the present study are similar and consist of three regions of absorption. The electronic spectrum of Bpmp shows two absorption bands 257 nm and 284 nm corresponding to $\pi \rightarrow \pi^*$ transition within the structure. The absorption bands of the complex **1** and **2** are

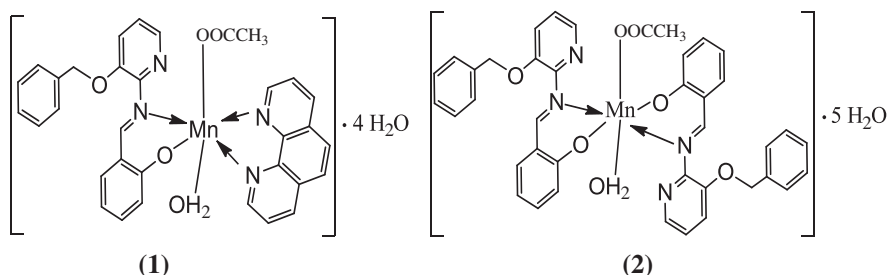


Fig. 1. Proposed structure of the complexes **1** and **2**.

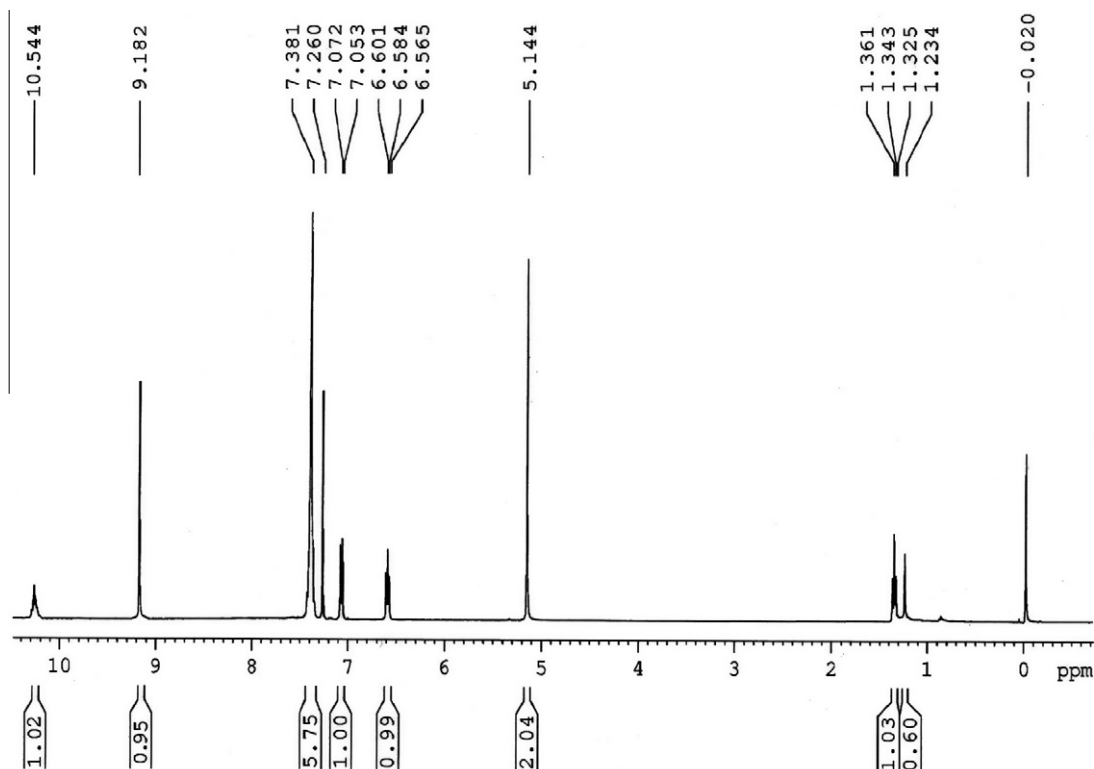


Fig. 2. ^1H NMR spectrum of the of the Bpmp.

shifted to longer wavelength region 278–283 nm and 298–304 nm compared to the ligand. The bands appearing later at the low energy side are attributable to $n \rightarrow \pi^*$ transitions associated with the azomethine chromophores. The band obtained at ca. 412–426 nm region may be attributed to phenolate $\text{O}(\pi\pi) \rightarrow \text{Mn}(d\pi^*)$ ligand-to-metal charge transfer by analogy with some similar manganese(III) complexes [44]. Two bands with shoulders have been found around 520–626 nm suggesting an octahedral geometry, with the ${}^6\text{A}_{1g} \rightarrow {}^4\text{T}_{1g}$ (${}^4\text{G}$), ${}^6\text{A}_{1g} \rightarrow {}^4\text{T}_{2g}$ (${}^4\text{G}$) transition for complexes. These bands are reasonably assignable to d–d transition on the basis of their low extinction coefficients [45].

Magnetic measurements

The magnetic susceptibility data for manganese(III) complexes **1** and **2** found to be 4.73 and 4.95 BM, respectively, indicating high spin magnetically dilute d^4 configurations (t_{2g}^3, e_g^1). This value is expected for four unpaired electrons and lack of any kind of exchange interaction [46]. Mn(II) has undergone aerial oxidation to Mn(III) in both the complexes. This is probably due to the formation of more stable complexes by harder Mn(III) ion with ligands containing harder donor atoms [47]. The elemental analysis, the molar conductivity, the electronic spectra and the magnetic moments suggest an octahedral geometry for complexes **1** and **2**, with a coordinated water molecule and acetate ion in the axial positions.

Mass spectra

Mass spectra of all the compounds stand in good agreement with proposed structure, the representative mass spectra shown in Figs. S4–S6. A moderate peak at m/z 305 is due to the formation of Schiff base ($\text{Bpmp} + 1$) $^+$. A distinct but less abundant peak observed at ($m/z = 275$) due to elimination of CO from the parent compound. One intense peak at m/z 201 is due to the formation

of starting amine compound. Other fragments are in good agreement with the ligand structure. The FAB mass peak corresponds to the Schiff base complex (**1**) was appeared at $688 m/z$ ($M + 1$) $^+$. Mass spectrum of the complex **1** show molecular ion peak at $556 m/z$, for the ligands attached to metal center with one water molecule after elimination of acetate moiety [48]. Similarly, for complex **2** the peak at $680 m/z$ appeared corresponds to the ligand attached to metal center with one water molecule. The peak appeared at 688 and $829 m/z$ for the complexes **1** and **2** represents the structural formula $\{[\text{Mn}(\text{phen})(\text{Bpmp})(\text{CH}_3\text{COO})(\text{H}_2\text{O})]\cdot 4\text{H}_2\text{O}\}$ and $\{[\text{Mn}(\text{Bpmp})_2(\text{CH}_3\text{COO})(\text{H}_2\text{O})]\cdot 5\text{H}_2\text{O}\}$, respectively. These peaks match the weakly present lattice water molecules with metal ion, which is not unlikely. To confirm the presence of lattice H_2O molecules in the complexes, we carried out thermogravimetric analyses of complexes. However the coordinated ion acetate to metal was also supported by IR spectra. Other fragments are in good agreement with the complexes structure.

Thermal studies

Room temperature stability for the complexes **1** and **2** was revealed by its thermogravimetric study (Figs. S7 and S8) carried out from ambient temperature to 800°C in nitrogen atmosphere, at a heating rate of $10^\circ\text{C}/\text{min}$. The TGA indicated that complexes **1** and **2** lose $\sim 20\%$ and $\sim 19\%$ of the total weight in the 35 – 209°C temperature range, respectively. This weight loss corresponds to the release of lattice, as well as coordinated water molecules and one coordinated acetate ion (calcd., 21.68% and 20.16%, for **1** and **2**, respectively) [49]. When the temperature hold on rising, the complex **1** loses $\sim 70\%$ of the total weight in the 220 – 800°C temperature range, corresponding to the removal of phenanthroline moiety followed by Bpmp (calcd. 70.20%) and finally the formation of the residue. In complex **2**, the second stage of weight loss (calcd., 73.1%; found, $\sim 72\%$) occurs between 215 – 600°C , corresponding to

the removal of two Bpmp thereby leading to the formation of metal oxides.

Superoxide dismutase activity

Different methods (nonenzymatic and enzymatic methods) can be used to ascertain the superoxide radical scavenging activity of various compounds. The SOD-like activity for the reaction of different mimics was determined studying the effect of the complexes on superoxide generated by the NADH/PMS system as described in experimental section. This method is very sensitive for evaluation of superoxide radical scavenging activity and was used to calculate the IC_{50} of the active compounds (Table 1). As the reaction proceeds, the farmazan color is developed and a color change from yellow to blue, which was associated with an increase in the absorbance at 560 nm.

Complexes **1** and **2** show good SODs activity (Fig. 3) with respect to the standard complexes [50]. Under the reaction conditions used, the O_2^- radicals activity was almost completely inhibited by **1** at a concentration of $9.6 \mu\text{M}$ ($IC_{50} = 4.2 \mu\text{M}$). Complex **2** inhibited at the concentration of $7.5 \mu\text{M}$ ($IC_{50} = 3.4 \mu\text{M}$). The SODs activity of the present complexes **1** and **2** may be consistent with the replacement of only one inner-sphere water molecule and phosphate binding in a monodentate manner. From this observation one can presume that the SODs activity of **1** and **2** are not so strongly affected by phosphate, because there is still one labile acetate ion present in its sixth coordinate environment, which can be easily replaced by superoxide [51]. It cannot be ruled out that, the reason for the observed SODs activity of **1** and **2** is may be the presence of Mn(III)salen entity itself, not just the results of free manganese species potentially present in the solution [20]. The IC_{50} value exhibited by SODs **1** and **2** is lower than those reported for the standard Mn(III)-SODm, nevertheless, further systematic studies like kinetic effect of complexes on catalytic cycle of superoxide dismutation are in progress.

DNA binding study

Electronic absorption titration

Electronic absorption spectroscopy is widely employed to determine the propensity for binding of the complexes to calf thymus DNA (CT-DNA). Hypochromism happens when the DNA-binding mode of a complex has an electrostatic effect or an intercalation which stabilizes the DNA duplex [52]. The absorption spectra of the complexes **1** and **2** in the absence and presence of CT-DNA are shown in Fig. 4a and b. With increasing CT-DNA concentration, for complex **1**, the hypochromism in the band at 304 nm reaches as high as 34.7% with a small bathochromism of 4 nm. Complex **2** also shows an evident hypochromism of about 29.2% at 298 nm and bathochromism of about 2 nm. These spectroscopic characteristics suggest that these two complexes interact with DNA most likely through a mode that involves a stacking interaction between the aromatic chromophore and the base pairs of DNA [53]. If the binding mode is intercalation, the π^* orbital of the intercalated ligand can couple with the π orbital of the DNA

Table 1
SODs activity of complexes **1** and **2** in IC_{50} (μM).

Compounds	Suppression ratio, IC_{50} (μM)	Reference
EUK-189	1.4	[45]
MnL7	2.1	[45]
Complex 1	4.2	This work
Complex 2	3.4	This work
Mn(CH ₃ COO) ₂ ·4H ₂ O	No activity ^a	This work

^a Checked up to 200 μM .

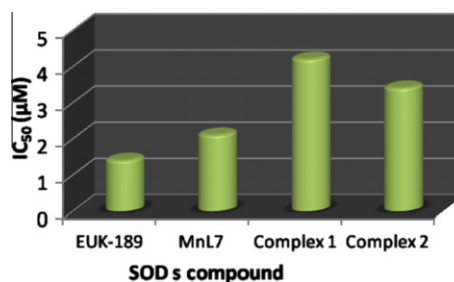


Fig. 3. Comparison of SODs activity of complexes **1** and **2** with standard SOD mimetic in IC_{50} value.

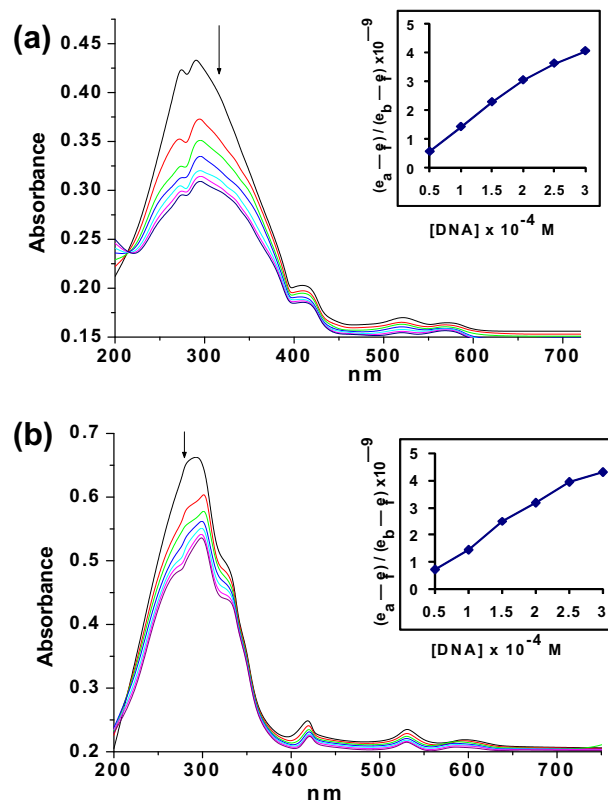


Fig. 4. Variation in the absorption spectra of complexes **1** (a) and **2** (b) in Tris-HCl buffer upon addition of increasing concentration of CT-DNA [0–300 μM]. [Complex] = 50 μM .

base pairs, thus, decreasing the $\pi \rightarrow \pi^*$ transition energy and resulting in the bathochromism. To compare quantitatively the affinity of the two complexes toward DNA, the intrinsic binding constants K_b of the two complexes to CT-DNA were determined by monitoring the changes of absorbance, with increasing concentration of DNA. The intrinsic binding constant K_b of complexes **1** and **2** obtained were $6.06 \times 10^4 \text{ M}^{-1}$ and $1.09 \times 10^4 \text{ M}^{-1}$, respectively, which is lower than that reported for classical intercalator (for ethidium bromide and [Ru(phen)DPPZ] whose binding constants have been found to be in the order of 10^6 – 10^7 M^{-1}) [54,55] and comparable with those reported for manganese complexes $\{[\text{MnCl}(\text{bpma})]_2[\text{Mn}(\mu\text{-Cl})_4(\text{H}_2\text{O})_2]\} \cdot \text{CH}_3\text{CN}$ ($1.37 \times 10^4 \text{ M}^{-1}$) [56] and $[\text{MnL}(\text{pic})_2] \cdot \text{H}_2\text{O}$ ($4.35 \times 10^4 \text{ M}^{-1}$) [57]. Comparing the intrinsic binding constant of the two complexes, we can deduce that both complexes bind to DNA by partial intercalation. However, the binding strength of complex **1** is greater than that of complex **2**. The additional planar aromatic moiety (phen) in the manga-

nese(III) complex **1**, may facilitate its potential intercalative DNA binding.

Competitive studies with EB

In general, measurement of the ability of a complex to affect the EB fluorescence intensity in the EB-DNA adducts allows determination of the affinity of the complex for DNA, whatever the binding mode may be. If a complex can replace EB from DNA-bound EB, the fluorescence of the solution will be quenched due to the fact that free EB molecules are readily quenched by the surrounding water molecules [58]. Two mechanisms have been proposed to account for this reduction in the emission intensity: the replacement of molecular fluorophores (EB in this case) and/or electron transfer [59]. For all the synthesized compounds, no emission was observed either alone or in the presence of CT-DNA in the buffer. A competitive binding of the Mn(III) complexes to CT DNA resulted in the reduction of the emission intensity due to displacement of bound EB. The quenching of the emission spectra of EB bound to DNA by the complexes **1** and **2** are shown in Fig. 5a and b. According to the classical Stern–Volmer equation [29], $I_0/I = 1 + K_{SV} [Q]$; I_0 and I are the fluorescence intensities in absence and in presence of the quencher, respectively. K_{SV} is a linear Stern–Volmer quenching constant, $[Q]$ is concentration of the quencher. The quenching of EB bound to CT-DNA by both complexes is in good agreement with the linear Stern–Volmer equation, which provides further evidence that the complexes bind to DNA. The K_{SV} values for complexes **1** and **2** are $1.02 \times 10^4 \text{ M}^{-1}$ and $6.6 \times 10^3 \text{ M}^{-1}$, respectively. The data suggest that the interaction of complex **1** with CT-DNA is stronger than that of complex **2**, which is consistent with the above absorption spectral results. The difference in

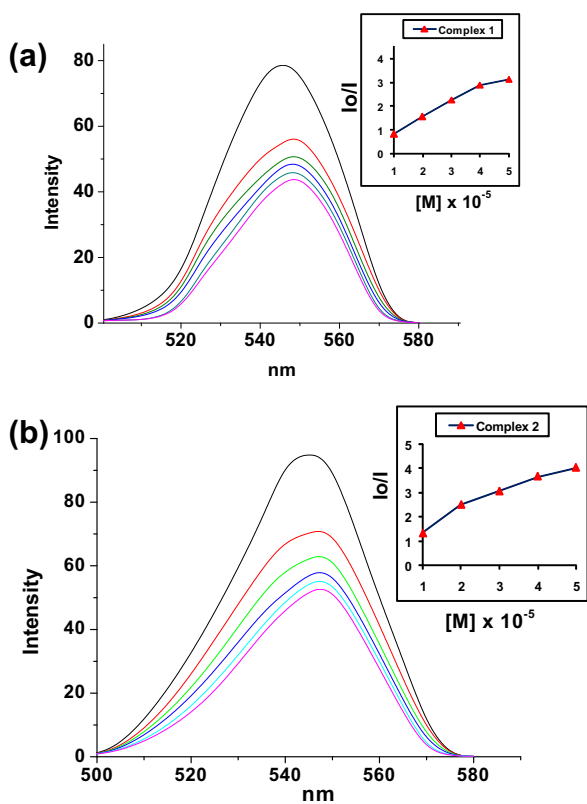


Fig. 5. Emission spectra of EB bound to DNA in the presence of increasing (a) complex **1** and (b) complex **2** concentration ($[EB] = 10 \mu\text{M}$, $[DNA] = 10 \mu\text{M}$, $[complex] = 0\text{--}50 \mu\text{M}$, $\lambda_{ex} = 376 \text{ nm}$; $\lambda_{em} = 545 \text{ nm}$ for complexes **1** and **2** respectively); Inset: Stern Volmer plot of I_0/I vs. $[complex]$ for the titration of the complexes to DNA-bound EB system.

quenching efficiency of complexes **1** and **2** may be due to the interaction of former with DNA through additional planar aromatic phen moiety, so releasing some free EB from the EB–DNA complex.

Viscosity measurements

Furthermore, the interactions between the complexes and DNA were investigated by viscosity measurements. In the absence of X-ray structural data, viscosity measurement is regarded as the most effective means to study intercalative binding mode of DNA in solution [60]. A classical intercalative mode causes significant increase in viscosity of the DNA solution due to an increase in separation of base pairs at the intercalation sites and hence an increase in overall DNA length. In contrast, a partial, non-classical intercalation of ligand could bend (or kink) the DNA helix, reduce its effective length and, concomitantly, its viscosity [61]. Fig. 6 shows the viscometric titration results of complexes **1** and **2** towards CT DNA. The viscosity of CT DNA increases with increase in the ratio of **1** and **2** to CT DNA, also this result resembles the binding mode of EB to CT DNA. These results also suggested that both of the compounds could bind to DNA in an intercalative mode. Notably, **1** caused a greater extent of viscosity changes, indicating the stronger binding ability than that of **2**. This result was also consistent with those obtained in fluorescent and electronic absorption titration measurements.

DNA cleavage efficiency studies

It is known that DNA cleavage activity is proceeds by relaxation of supercoiled circular conformation of plasmid DNA to nicked circular and/or linear conformation. When electrophoresis is applied to circular plasmid DNA, fastest migration will be observed for DNA of closed circular conformations (Form I). If one strand is cleaved, the supercoiled will relax to produce a slower moving nicked conformation (Form II). If both strands are cleaved, a linear conformation (Form III) will be generated and migrates in between [62]. Incubating plasmid pUC19 DNA with the increasing amounts of the complex concentration of 100, 200, 300 and 400 μM , in presence of oxidizing agent H_2O_2 under physiological conditions produced the outcome shown in Fig. 7. The results show that both complexes **1** and **2** behave as a chemical nucleases by nicking the DNA Form I into Form II, at the concentration of 100 μM . The increasing concentrations of complexes led to a gradual diminish in the band intensity of Form I, while increasing Form II progressively suggesting single strand DNA cleavage. In contrast, the starting material Mn(II) acetate salt does not seemed to cleave the DNA at 400 μM (data not showed). Poor cleavage of DNA was observed on incubation of complexes **1** and **2** in the absence of hydrogen

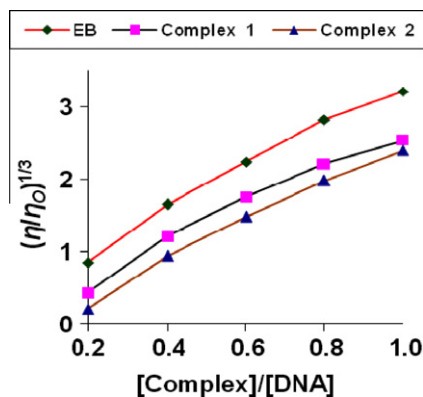


Fig. 6. Effect of increasing the concentration of the complexes **1** (■), **2** (▲), and EB (◆) on the relative viscosities of CT-DNA at $28.0 \pm 0.1 \text{ }^\circ\text{C}$ in 5 mM Tris–HCl buffer (pH 7.2).

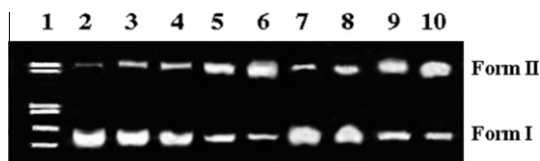


Fig. 7. Cleavage picture of SC pUC19 DNA (30 μM) by different concentration of complexes **1** and **2** (100–400 μM) in 10 mM Tris-HCl/1 mM EDTA buffer (pH 8.0).

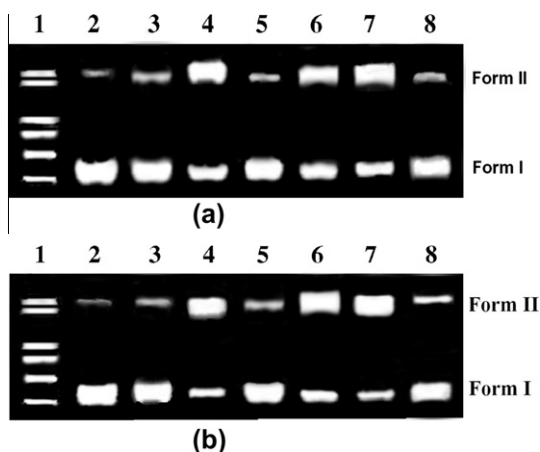


Fig. 8. Cleavage of SC pUC19 DNA (30 μM) by complexes **1** (a) and **2** (b) (400 μM) in the presence of H_2O_2 (100 μM), in 10 mM Tris-HCl/1 mM EDTA buffer (pH 8.0). The strong inhibitions of DNA cleavage to complexes was observed in the presence of the hydroxyl radical scavenger DMSO and their ability of groove binding.

peroxide (data not showed). This indicates that hydrogen peroxide plays a role to aid the complexes in DNA degradation by oxidative cleavage, and engages in an oxidation reaction on the DNA strand. This result is comparable with previous studies of DNA cleavage by other Manganese complexes where hydrogen peroxide is needed and reactive hydroxyl radicals are involved [63,64].

Furthermore, in order to investigate the nature of reactive species that is responsible for the cleavage of the plasmid DNA by **1** and **2**, reaction was carried out with standard radical scavengers,

viz. DMSO as hydroxyl radical scavengers, NaN_3 as singlet oxygen quencher under identical conditions (Fig. 8a and b). This experiment reveals that DMSO inhibits the DNA cleavage to the maximum caused by **1** and **2**, suggesting the involvement of hydroxyl radicals in the cleavage process. On the other hand the complexes show no inhibition in the DNA cleavage activity in the presence of singlet oxygen quencher NaN_3 . Therefore, the presence of singlet oxygen should be ruled out of the DNA cleavage process. Thus, the catalytic pathway for the DNA cleavage mechanism by complexes **1** and **2** is a hydrolytic cleavage process [65].

In order to study the binding of the complexes to pUC19 DNA, the major groove binder methyl green and the minor groove binder distamycin were added prior to the addition of the complexes to DNA [66]. Methyl green was found to inhibit the DNA breakage mediated by both complexes (lane 8, Fig. 8a and b). In contrast, distamycin had no effect on the cleavage produced by both complexes (Fig. 8a and b, lane 7). These findings suggest that the complexes prefer to bind through the major groove only.

Antimicrobial activities

Antimicrobial drugs are designed to inhibit/kill the infecting organisms and to have no minimal effect on the recipient. Manganese is better against antimicrobial activity with low toxicity and high selectivity than nickel, copper, titanium, zirconium, silver, cadmium and zinc. Maneb, the coined name for manganese ethylene bis-dithiocarbamate has been used as commercial fungicide, against a wide variety of diseases particularly of vegetable and fruits [67]. The results of the antimicrobial activity have been compared with the conventional fungicide Fluconazole and the bactericide Chloramphenicol used as the standards. The results achieved from these studies have been enlisted in Tables 2 and 3. The data of the anti-fungal and antibacterial activity indicated that the metal chelates are more active than the ligands. However, the increased biocidal properties after complexation can be very well explained by chelation theory [68]. The mechanism of the toxicity of the complexes with the ligands may be ascribed to the increase of the lipophilic nature of the complexes arising from chelation. Due to the complexity of biological system, it is rather difficult to stipulate the exact mechanism for such activities.

Table 2
Antimicrobial results of Hbid and its metal complexes.

Compounds	% Inhibition against bacteria ^a				% Inhibition against fungi ^a	
	<i>S. aureus</i>	<i>X. vesicatoria</i>	<i>R. solanacearum</i>	<i>E. coli</i>	<i>A. niger</i>	<i>A. flavus</i>
Bpmp	32	26	36	25	34	36
Complex 1	36	33	46	30	45	48
Complex 2	34	30	42	30	44	46
Chloramphenicol	100	100	100	100	–	–
Fluconazole	–	–	–	–	100	100

^a The results obtained were the average of three replicates.

Table 3
Minimum inhibitory concentration results in ($\mu\text{g}/\text{mL}$).

Compound	IC_{50} ($\mu\text{g}/\text{mL}$) ^a					
	<i>S. aureus</i>	<i>X. vesicatoria</i>	<i>R. solanacearum</i>	<i>E. coli</i>	<i>A. niger</i>	<i>A. flavus</i>
Bpmp	>100	>100	>100	>100	>100	>100
Complex 1	75	65	60	80	55	50
Complex 2	70	80	55	85	60	55
Chloramphenicol	<20	20	<20	20	–	–
Fluconazole	–	–	–	–	20	20

^a The results obtained were the average of three replicates.

The susceptibilities of all strains of bacteria and a fungus to the Bpmp and its corresponding mononuclear manganese complexes were evaluated by measuring the minimum inhibitory concentration at which no growth was observed was taken as the MIC values. Comparison of MIC values (in $\mu\text{g}/\text{mL}$) of Bpmp, Mn(III) complexes and standard drugs against different bacteria are presented in Table 3. The results indicated that, these compounds were active in inhibiting the growth of tested organisms starting from 50 $\mu\text{g}/\text{mL}$ concentration. Complexes **1** and **2** appeared to have broad spectrum as it exhibit mild to moderate activity towards most of the strains. This study suggests that these complexes can further be explored as specific antimicrobial drugs due to their polite activity and less toxicity of metal ion.

Conclusion

On the basis of above studies, the general structure of the Mn(III) complexes are proposed as shown in Fig. 1. The complexes having distorted octahedral geometry with N, O as donor site from Schiff base and N, N contributed from the neutral ligand o-phenanthroline. Monodentate nature of anion acetate confirmed from the FT-IR and indicates coordination with metal ion. The Mn(III) oxidation state in **1** and **2** is highly stabilized by two Bpmp ligands. Thus Bpmp could be used as a chelator for the removal of excess intracellular Mn and the treatment of chronic Mn toxicity. *In vitro* DNA binding studies reveal that the complexes bind to the DNA helix via the partial intercalative interaction. The complexes **1** and **2** bind to supercoiled plasmid pUC19 DNA in major groove and displays efficient hydrolytic cleavage. The salen–manganese complexes **1** and **2** represent a new class of potential clinical agents. The order of SODs like activities observed from spectroscopic assays is (**2**) > (**1**). Moreover biological screening state that Schiff base complexes enhance the activity against the bacteria and fungi due to complexes bearing polar properties, and this study helps to evaluate the potentiality and effectiveness of newer Mn(III) complexes to use as antibacterial agents.

Acknowledgments

The author L. Shiva Kumar is thankful to the UGC, New Delhi for the award of Rajiv Gandhi National Fellowship. We also thank Head of the Department of Biotechnology, University of Mysore, for providing the help in carrying out antimicrobial and nuclease activities.

Appendix A. Supplementary material

Supplementary data associated with this article can be found, in the online version, at <http://dx.doi.org/10.1016/j.saa.2013.01.025>.

References

- [1] G.W. Yang, X.P. Xia, H. Tu, C.X. Zhao, Chem. Res. Appl. 7 (1995) 41–52.
- [2] V.L. Pecoraro, W.-Y. Hsieh, in: A. Sigel, H. Sigel (Eds.), Metal Ions in Biological Systems: Manganese and its Role in Biological Processes, vol. 37, Marcel Dekker, New York, 2000, p. 431.
- [3] R. Ji, K. Yu, L.L. Lou, C. Zhang, Y. Han, S. Pan, S. Liu, Inorg. Chem. Commun. 25 (2012) 65–69.
- [4] T. Katsuki, Coord. Chem. Rev. 140 (1995) 189–214.
- [5] W. Li, Z. Li, L. Li, D. Liao, Z. Jiang, J. Solid State Chem. 180 (2007) 2973–2977.
- [6] A. Puglisi, G. Tabbi, G. Vecchio, J. Inorg. Biochem. 98 (2004) 969–976.
- [7] S. Majumder, S. Hazra, S. Dutta, P. Biswas, S. Mohanta, Polyhedron 28 (2009) 2473–2479.
- [8] J.J.R. Frausto da Silva, R.J.P. Williams, The Biological Chemistry of the Elements, Clarendon Press, Oxford, 1993, p. 4.
- [9] S.R. Doctrow, K. Huffman, C.B. Marcus, C. Tocco, E. Malfroy, C.A. Adinolfi, H. Kruk, K. Baker, N. Lazarowich, J. Mascarenhas, B. Malfroy, J. Med. Chem. 45 (2002) 4549–4558.
- [10] W. Park, D. Lim, Bioorg. Med. Chem. Lett. 19 (2009) 614–617.
- [11] W.-Y. Hsieh, S. Liu, Inorg. Chem. 44 (6) (2005) 2031–2038.
- [12] (a) J.J.R. Frausto da Silva, R.J.P. Williams, The Biological Chemistry of the Elements, Oxford University Press, 2001; (b) V.L. Pecoraro (Ed.), Manganese Redox Enzymes, VCH, New York, 1992.
- [13] I. Sakiyan, E. Logoglu, S. Arslan, N. Sari, N. Sakiyan, BioMetals 17 (2004) 115–120.
- [14] C.D. Samara, A.N. Papadopoulos, D.A. Malamatar, A. Tarushi, C.P. Raptopoulou, A. Terzis, E. Samaras, D.P. Kessissoglou, J. Inorg. Biochem. 99 (2005) 864–875.
- [15] Y.-P. Li, P. Yang, Inorg. Chem. Commun. 14 (2011) 545–549.
- [16] M.N. Dehkordi, A.K. Bordbar, M.A. Mehrgardi, V. Mirkhani, J. Fluoresc. 21 (2011) 1649–1658.
- [17] S.S. Mandal, U. Varshney, S. Bhattacharya, Bioconjugate Chem. 8 (6) (1997) 798–812.
- [18] I. Fridovich, Annu. Rev. Biochem. 64 (1995) 97–112.
- [19] G. Lupidi, F. Marchetti, N. Masciocchi, D.L. Reger, S. Tabassum, P. Astolfi, E. Damiani, C. Pettinari, J. Inorg. Biochem. 104 (2010) 820–830.
- [20] F.C. Friedel, D. Lieb, I. Ivanovic-Burmazovic, J. Inorg. Biochem. 109 (2012) 26–32.
- [21] J. Prousek, Pure Appl. Chem. 79 (2007) 2325–2338.
- [22] M.J. Daly, E.K. Gaidamakova, V.Y. Matrosova, A. Vasilenko, M. Zhai, A. Venkateswaran, M. Hess, M.V. Omelchenko, H.M. Kostandarites, K.S. Makarova, L.P. Wackett, J.K. Fredrickson, D. Ghosal, Science 306 (2004) 1025–1028.
- [23] D.P. Riley, Chem. Rev. 99 (1999) 2573–2587.
- [24] W. Jiang, Y. Han, Q. Pan, T. Shen, C. Liu, J. Inorg. Biochem. 101 (2007) 667–677.
- [25] M. Devereux, D.O. Shea, A. Kellett, M. McCann, M. Walsh, D. Egan, C. Deegan, K. Kedziora, G. Rosair, H. Muller-Bunz, J. Inorg. Biochem. 101 (2007) 881–892.
- [26] D.D. Perrin, W.L.F. Armarego, D.R. Perrin, Purification of Laboratory Chemicals, second ed., Pergamon Press, Oxford, 1980.
- [27] A.I. Vogel, A Text Book of Quantitative Chemical Analysis, fifth ed., Longman, London, 1989.
- [28] P. Kakkar, B. Das, P.N. Viswanathan, Ind. J. Biochem. Biophys. 21 (1984) 130–132.
- [29] S. Satyanarayana, J.C. Dabrowiak, J.B. Chaires, Biochemistry 32 (1993) 2573–2584.
- [30] S. Banerjee, S. Mondal, W. Chakraborty, S. Sen, R. Gachhui, R.J. Butcher, A.M.Z. Slawin, C. Mandal, S. Mitra, Polyhedron 28 (2009) 2785–2793.
- [31] A. Wolfe, G.H. Shimer, T. Meehan, Biochemistry 26 (1987) 6392–6396.
- [32] J.B. Chaires, N. Dattagupta, D.M. Crothers, Biochemistry 21 (1982) 3933–3940.
- [33] G. Cohen, H. Eisenberg, Biopolymers 8 (1969) 45–55.
- [34] J.B. Suffredini, H.S. Sader, A.G. Goncalves, A.O. Reis, A.C. Gales, A.D. Varella, R.N. Younes Brazil, J. Med. Biol. Res. 37 (2004) 379–384.
- [35] G.S. Girolami, T.B. Rauchfuss, R.J. Angelici, Synthesis and Technique in Inorganic Chemistry, third ed., University Science Books, Sausalito, 1999, p. 254.
- [36] O. Poulalimardan, A.C. Chamayou, C. Janiak, H. Hosseini-Monfared Inorg. Chim. Acta 360 (2007) 1599–1608.
- [37] K.R. Surati, B.T. Thaker, S.L. Oswal, R.N. Jadeja, V.K. Gupta, Struct. Chem. 18 (2007) 295–310.
- [38] M. Salavati-Niasari, Z. Salimi, M. Bazarganipour, F. Davar, Inorg. Chim. Acta 362 (2009) 3715–3724.
- [39] R. Karmakar, R.C. Choudhury, G. Bravic, J.P. Sutter, S. Mitra, Polyhedron 23 (2004) 949–954.
- [40] S. Belaid, A. Landreau, S. Djebbar, O. Benali-Baitich, G. Bouet, J.P. Bouchara, J. Inorg. Biochem. 102 (2008) 63–69.
- [41] K. Nakamoto, Infrared and Raman Spectra of Inorganic and Coordination Compounds, fifth ed., J. Wiley, New York, 1997.
- [42] D.P. Singh, K. Kumar, C. Sharma, Eur. J. Med. Chem. 45 (2010) 1230–1236.
- [43] A. Neves, S.M.D. Erthal, I. Vencato, A.S. Ceccato, Y.P. Mascarenhas, O.R. Nascimento, M.H. Corner, A.A. Batista, Inorg. Chem. 31 (1992) 4749–4755.
- [44] M. Bera, K. Biradha, D. Ray, Inorg. Chim. Acta 357 (2004) 3556–3562.
- [45] M. Matzapetakis, N. Karligiano, A. Bino, M. Dakanali, C.P. Raptopoulou, V. Tangoulis, A. Terzis, J. Giapintzakis, A. Salifoglou, Inorg. Chem. 39 (2000) 40–44.
- [46] K.R. Surati, B.T. Thaker, G.R. Shah, Synth. React. Inorg. Met.-Org. Nano-Met. Chem. 38 (2008) 272–279.
- [47] Z. Lu, M. Yuan, F. Pan, S. Gao, D. Zhang, D. Zhu, Inorg. Chem. 45 (2006) 3538–3548.
- [48] K.R. Surati, B.T. Thaker, Spectrochim. Acta (A) 75 (2010) 235–242.
- [49] K.R. Surati, Spectrochim. Acta (A) 79 (2011) 272–277.
- [50] O. Iranzo, Bioorg. Chem. 39 (2011) 73–87.
- [51] B. Drahos, J. Kotek, P. Herman, I. Lukes, E. Tóth, Inorg. Chem. 49 (2010) 3224–3238.
- [52] P. Yang, M.L. Guo, B.S. Yang, Chin. Sci. Bull. 39 (1994) 997.
- [53] B. Peng, Z. Wen-Hui, L. Yan, L. Han-Wen, L. Zhu, Transition Met. Chem. 34 (2009) 231–237.
- [54] M. Waring, J. Mol. Biol. 13 (1965) 269–282.
- [55] L. Chen, J. Liu, J. Chen, C. Tan, J. Inorg. Biochem. 102 (2008) 330–341.
- [56] J. Qian, X.F. Ma, H.Z. Xu, J.L. Tian, J. Shang, Y. Zhang, S.P. Yan, Eur. J. Inorg. Chem. 2010 (20) (2010) 3109–3116.
- [57] H. Wu, J. Yuan, Y. Bai, H. Wang, G. Pan, J. Kong, J. Photochem. Photobiol., B: Biol. 116 (2012) 13–21.
- [58] J.B. LePecq, C. Paoletti, J. Mol. Biol. 27 (1967) 87–106.
- [59] R.F. Pasternack, M. Cacca, B. Keogh, T.A. Stephenson, A.P. Williams, F.J. Gibbs, J. Am. Chem. Soc. 113 (1991) 6835–6840.
- [60] B.C. Baguley, M. Lebre, Biochemistry 23 (1984) 937–943.

- [61] Qiang Liu, Ji Zhang, Ming-Qi Wang, Da-Wei Zhang, Lu Qiao-Sen, Yu Huang, Hong-Hui Lin, Yu Xiao-Qi, *Eur. J. Med. Chem.* 45 (2010) 5302–5308.
- [62] G. Psomas, *J. Inorg. Biochem.* 102 (2008) 1798–1811.
- [63] K. Ghosh, N. Tyagi, P. Kumar, U.P. Singh, N. Goel, *J. Inorg. Biochem.* 104 (2010) 9–18.
- [64] F. Arjmand, S. Parveena, M. Afzal, L. Toupet, T.B. Hadda, *Eur. J. Med. Chem.* 49 (2012) 141–150.
- [65] J. Lu, H.Y. Liu, L. Shi, X. Li Wang, X. Ying, L. Zhang, L. Nian Ji, L.Q. Zang, C.K. Chang, *Chin. Chem. Lett.* 22 (2011) 101–104.
- [66] S. Tabassum, M. Zaki, F. Arjmand, I. Ahmad, *J. Photochem. Photobiol., B: Biol.* 114 (2012) 108–118.
- [67] Y.L. Nene, P.N. Thapliyal, *Fungicides in Plant Disease Control*, second ed., Oxford and IBH Publishing Co., 1979.
- [68] R.V. Singh, A. Chaudhary, *J. Inorg. Biochem.* 98 (2004) 1712–1721.